

Ion fluxes and energies in inductively coupled radio-frequency discharges containing C_2F_6 and $c-C_4F_8$

A. N. Goyette,^{a)} Yicheng Wang, M. Misakian, and J. K. Olthoff

Electricity Division, Electronics and Electrical Engineering Laboratory, National Institute of Standards and Technology, Gaithersburg, Maryland 20899-8113

(Received 4 February 2000; accepted 17 July 2000)

We report ion energy distributions (IEDs), relative ion intensities, and absolute total ion current densities at the grounded electrode of an inductively coupled Gaseous Electronics Conference (GEC) radio-frequency (rf) reference cell for discharges generated in pure C_2F_6 , $c-C_4F_8$, and in mixtures of each gas with Ar. These discharges contain several ions of significant intensity, with the dominant ion seldom that expected from direct ionization of the feed gas. Neither the C_2F_6 nor the $c-C_4F_8$ fraction in the Ar mixtures significantly influences the reactive ion composition. IEDs vary from single peaked to bimodal, the latter indicating rf modulation of the ions' energy as they traverse the plasma sheath. Elevated gas pressures and higher fractions of either C_2F_6 or $c-C_4F_8$ all result in comparatively broader and more bimodal IEDs. IEDs in pure $c-C_4F_8$ discharges, compared to C_2F_6 discharges, generally exhibit more pronounced broadening and bimodality. [S0734-2101(00)01106-4]

I. INTRODUCTION

Low pressure radio-frequency (rf) discharges in fluorocarbon gases are commonly used for the plasma etching of semiconductor materials. Ion bombardment is a key process in plasma etching and consequently the determination of the identities, flux, and energies of the ions striking surfaces exposed to etching discharges has attracted much interest. Most investigations of positive ions in rf plasmas sustained in either C_2F_6 or $c-C_4F_8$ have been applied to capacitively coupled reactors,¹⁻³ and only recently have investigations been extended to inductively coupled reactors.^{4,5}

We report mass analyzed ion energy distributions (IEDs), relative ion flux densities, and absolute total ion currents measured using a combined ion energy analyzer-mass spectrometer that samples ions through an orifice in the lower electrode of an inductively coupled Gaseous Electronics Conference (GEC) rf reference cell. The absolute ion flux measurements and the ion energy distributions are the first reported for C_2F_6 and $c-C_4F_8$, and are useful for model validation. Ion energies and mass-resolved ion fluxes were measured as a function of gas pressure and mixture concentration. Data are presented for discharges generated in C_2F_6 , $c-C_4F_8$, and in mixtures of each gas with argon.

II. EXPERIMENT

The discharges studied were generated in a GEC rf reference cell reactor whose upper electrode has been replaced with a five-turn planar rf-induction coil behind a quartz window to produce inductively coupled discharges.⁶ The design of the GEC rf reference cell is described in detail elsewhere.^{7,8} In a manner similar to that of Jayaraman, McGrath, and Hebner,⁴ a quartz annulus was mounted to the upper quartz window of the GEC cell. This ring was developed for use in the GEC rf reference cell to allow the gen-

eration of plasmas in electronegative gases over a much broader range of pressures and powers. The reactor, along with the ion energy analyzer and mass spectrometer, are depicted schematically in Fig. 1. The feed gas enters the cell through one of the 2.75 in. side flanges and is pumped out through the 6 in. port attached to the turbo-molecular pump. The gas pressure is maintained by a variable gate valve between the GEC cell and the pump. Mass flow controllers regulated the flow, which was maintained at 3.73 $\mu\text{mole/s}$ (5 sccm) for pure C_2F_6 or $c-C_4F_8$ discharges or 7.45 $\mu\text{mole/s}$ (10 sccm) for different mixtures of C_2F_6 and $c-C_4F_8$ with Ar.

A 13.56 MHz voltage is applied to the coil through a matching network. The rf power values presented in this article are the net power to the matching network driving the coil. The actual rf power dissipated in the plasma has been determined to be approximately 80% of the power listed.⁶ The lower electrode is grounded to the vacuum chamber.

The ion sampling arrangement is identical to that used to study inductively coupled plasmas in CF_4 ,⁹ and in Ar, N_2 , O_2 , Cl_2 and their mixtures.¹⁰ Ions are sampled through a 10- μm -diam orifice in a 2.5- μm -thick nickel foil spot welded into a small counterbore located at the center of the stainless steel lower electrode. The 10 μm orifice allows more accurate measurement of relative ion flux intensities than larger orifices ($\geq 100 \mu\text{m}$) commonly used in capacitively coupled plasmas. For IED measurements, the ions that pass through the orifice are mass selected by the quadrupole mass spectrometer after being energy analyzed by the 45° electrostatic energy selector. The IEDs measured in this manner are essentially ion-flux energy distributions.¹¹

Past experience with the ion energy analyzer indicates that the ion transmission is nearly constant over the energy ranges observed here.¹¹ A mass-dependent transmission correction factor, however, was applied to the highest mass ions (mass > 40 u) in order to compensate for some decrease in the ion transmission of the quadrupole mass spectrometer with increasing mass. These factors were determined by cali-

^{a)}Electronic mail: goyette@eeel.nist.gov

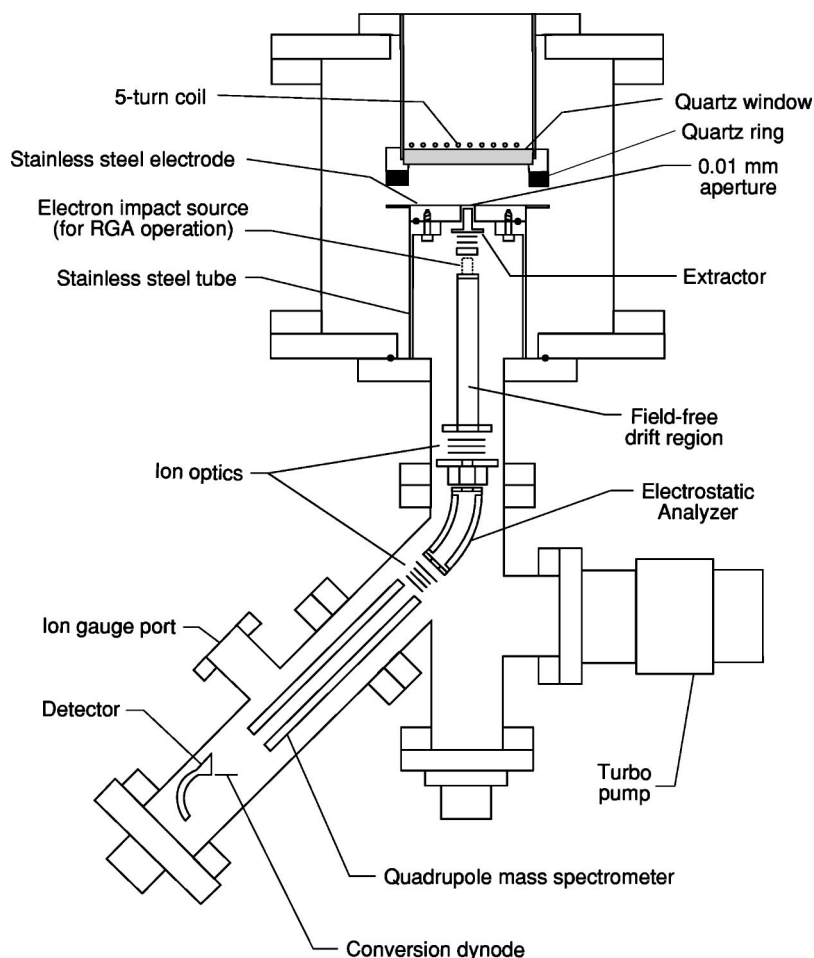


FIG. 1. Schematic diagram of the inductively coupled GEC rf reference cell reactor with the ion energy analyzer and mass spectrometer appended to the modified lower electrode.

bration with rare gas plasmas¹⁰ and approach a factor of 16 for the largest mass ion observed, $C_2F_5^+$ at 119 u.

For total ion current measurements, (i.e., all ion current passing through the sampling orifice), the ion optic elements at the front of the ion energy analyzer are biased such that the current passing through the sampling orifice is collected on the extractor element (the first ion optic element behind the electrode surface), and is measured using an electrometer. The electrometer registers a small residual current even when the discharge is off; this is subtracted from all ion currents measured from the discharge.

The total ion current is partitioned into mass channels according to the mass spectrum of ions. The absolute intensities of the measured IEDs are then determined by scaling the measured values of the ion current for the appropriate mass channel to the total ion current. The ion flux densities presented here are derived by dividing the total measured ion current by the area of the 10- μ m-diam sampling hole.

III. RESULTS AND DISCUSSION

A. C_2F_6

Figure 2(a) shows a mass spectrum of the ions produced in a pure C_2F_6 discharge at 1.33 Pa (10 mTorr) and 200 W. Similar to the observations of Jayaraman, McGrath, and Hebner⁴ and Li *et al.*,⁵ the dominant ion under these condi-

tions is CF_3^+ . With a measured flux equal to 30% of the total ion current, CF_3^+ is also the principal ion fragment produced from the dissociative ionization of C_2F_6 .¹² Jayaraman, McGrath, and Hebner⁴ report a flux of CF_3^+ five times higher than that of the next most abundant ion. In contrast, we observe that the intensities of CF^+ and CF_2^+ are nearly half that of CF_3^+ . Surprisingly, the second highest intensity in Fig. 2(a) is at mass 28 u, which can be attributed to the combined flux of CO^+ and Si^+ . Both CO^+ and Si^+ are secondary ions (ions not produced by dissociative ionization of the parent gas) resulting from quartz etching and subsequent ion-surface and ion-molecule interactions occurring within the reactor.

The isotopes of silicon have much higher abundances than those of either carbon or oxygen. Consequently, the isotopic abundance ratios of Si can be used to determine the contribution of $^{28}Si^+$ to the measured flux of 28 u ion fragments. If one assumes that the fluxes of 29 and 30 u ion fragments are entirely due to $^{29}Si^+$ and $^{30}Si^+$, respectively, the contribution of $^{28}Si^+$ to the measured flux of 28 u ion fragments is roughly half, with the remainder of the flux attributable to CO^+ . A similar analysis was performed for the measured fluxes of ions having masses corresponding to SiF_x^+ . These fluxes consist primarily of SiF_x^+ rather than COF_x^+ species. The presence of substantial fractions of ions containing Si

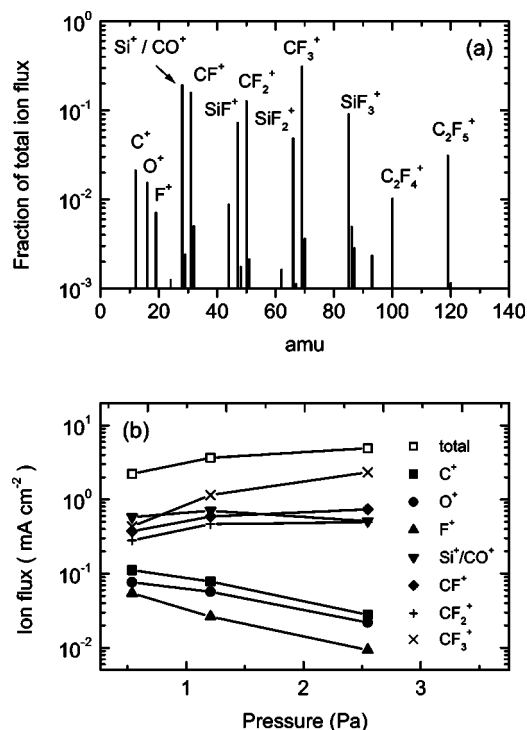


FIG. 2. (a) Mass spectrum of ions striking the lower electrode of the GEC cell in a C_2F_6 discharge at 1.33 Pa (10 mTorr) and (b) the mass analyzed ion flux striking the lower electrode as a function of discharge pressure. Discharge power is maintained at 200 W.

has similarly been observed in discharges containing CF_4 ,⁹ and in discharges containing CHF_3 .¹³ This is an important observation for discharge modeling and validation. Based on isotope analysis, the other significant ions from pure C_2F_6 discharges in order of decreasing abundance are CF^+ , CF_2^+ , SiF_3^+ and SiF_2^+ which combined comprise nearly 50% of the total ion current.

It is worth mentioning that Jayaraman, McGrath, and Hebner⁴ detected ions having masses corresponding to Si^+ and SiF_x^+ from their C_2F_6 discharges with significantly lower relative abundances. This is interesting considering the fact that bare and resist-covered Si wafers were present in their discharges, which would suggest a ready source of Si atoms. The differences in relative abundances of the various ions could be attributed to fundamental differences in the plasma conditions due to the absence of a wafer in our experiments. Another explanation, however, is differences caused by the dissimilar ion sampling geometries. Whereas we extracted ions through an orifice in the grounded lower electrode, Jayaraman, McGrath, and Hebner⁴ extracted ions from the side of the GEC cell between the lower electrode and the bottom of the quartz annulus. In the latter experimental configuration, the probe tip of the mass spectrometer is separated from the plasma by a relatively thick diffusion layer through which the primary ions must travel before detection. Thus they have a large probability of undergoing ion-molecule reactions, which may influence the relative abundances of the detected ions.

The relative ion composition as a function of pressure in

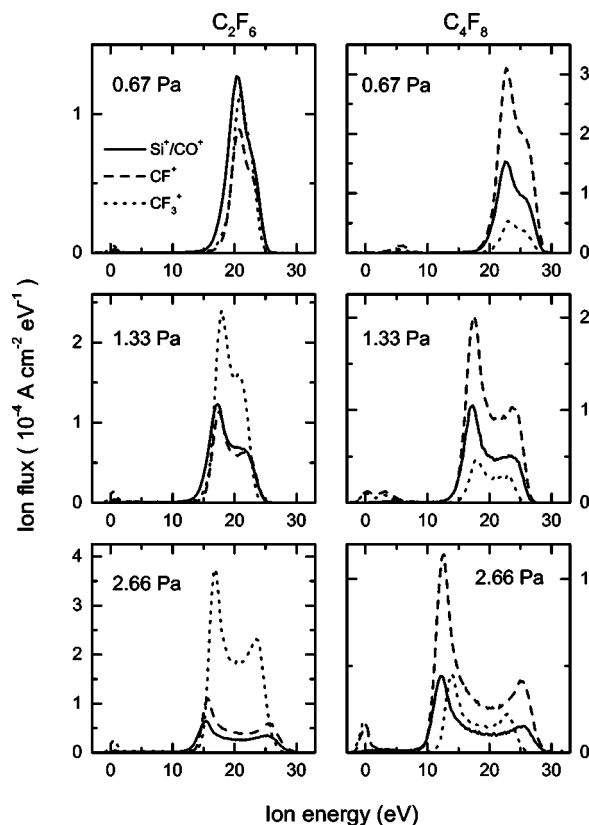


FIG. 3. Energy distributions of the three dominant ions produced in pure C_2F_6 and *c*- C_4F_8 discharges at 0.67, 1.33, and 2.66 Pa (5, 10, and 20 mTorr). The legend applies to all panels. Discharge power is maintained at 200 W.

pure C_2F_6 discharges is shown in Fig. 2(b). The magnitude of the total ion flux more than doubles from 0.67 to 2.66 Pa (5–20 mTorr). While the fluxes of the atomic ions decrease significantly in this range, the CF_3^+ flux rises dramatically, increasing by almost a factor of five. The fact that the CF_3^+ flux is such a strongly increasing function of gas pressure suggests that in addition to electron-impact ionization of C_2F_6 , reactions between ions and either C_2F_6 or dissociation fragments may be important mechanisms contributing to CF_3^+ production in these discharges. Little is known about such ion-molecule reactions, however.

The energy distributions of three significant ions in pure C_2F_6 discharges at 0.67, 1.33, and 2.66 Pa (5, 10, and 20 mTorr) are shown in the first column of Fig. 3. At the lowest pressure studied, the IEDs are fairly narrow, with approximately the same width and peak position. A small peak is also present near 0 eV, however, in the energy distributions of CF_3^+ . The fact that this low-energy peak appears only for specific ionic species implies that an ion dependent process such as charge-exchange production of slow ions near the sampling orifice is responsible. At 1.33 Pa (10 mTorr), the IEDs are significantly broader and exhibit a readily seen splitting indicative of increased rf modulation of the ions' energy as they are accelerated across the plasma sheath.^{14,15} If the ion transit time through the sheath is sufficiently short compared to the rf period, then the ion energy averaged over

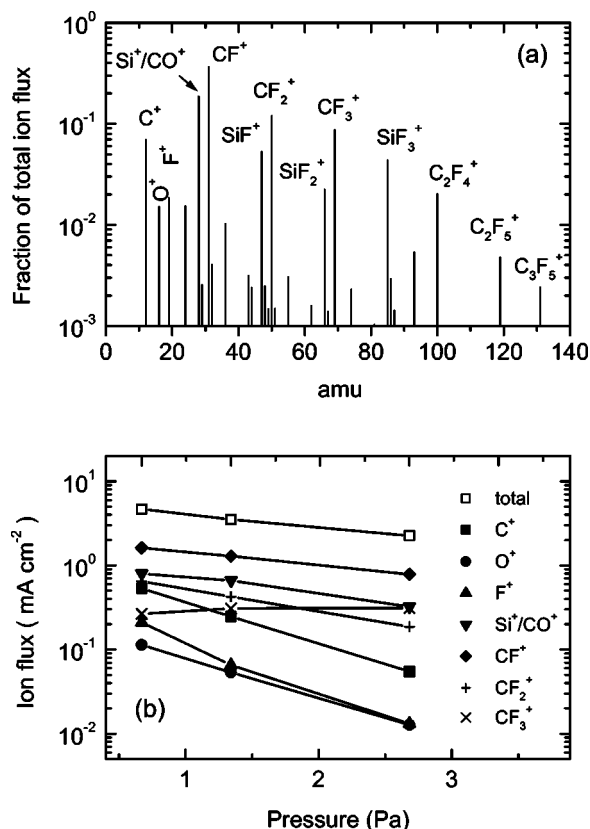


FIG. 4. (a) Mass spectrum of ions striking the lower electrode of the GEC cell in a 1.33 Pa (10 mTorr) $c\text{-C}_4\text{F}_8$ discharge and (b) the mass analyzed ion flux striking the lower electrode as a function of discharge pressure. Discharge power is maintained at 200 W.

an rf cycle becomes strongly modulated. The increase of rf modulation with pressure can be attributed to the decrease of the ground sheath capacitance resulting from a more confined plasma as the pressure increases. At 2.66 Pa (20 mTorr), the IEDs are even broader, and are distinctly bimodal in shape.

The appearance of mass-dependent structure in the energy distributions illustrates the importance of measuring IEDs when determining relative ion flux intensities with the type of instrument used in this study. Under conditions such as ours, relative ion intensity measurements that utilize simple mass scans will be affected by the energy setting of the energy analyzer. The measuring and integrating of IEDs is critical in determining accurate relative ion flux intensities. During the course of these experiments, care was taken when determining relative ion flux intensities to sample ions at energies corresponding to the means of the IEDs.

B. $c\text{-C}_4\text{F}_8$

A mass spectrum of the ions produced in a pure $c\text{-C}_4\text{F}_8$ discharge at 1.33 Pa (10 mTorr) and 200 W is shown in Fig. 4(a). Constituting nearly 35% of the total ion flux, CF^+ dominates the ion spectrum under these conditions. Other significant ions present include Si^+ , CO^+ , CF_2^+ , and CF_3^+ , which combined account for almost 40% of the ion current.

A similar analysis of the flux intensities of the ions containing isotopes of Si indicates the contribution of $^{28}\text{Si}^+$ to the measured flux of 28 u ion fragments is approximately half, with the remainder of the measured flux similarly attributable to CO^+ . The fluxes of ions having masses corresponding to SiF_x^+ are nearly entirely attributable to SiF_x^+ species rather than to COF_x^+ species. It is interesting to note that the relative intensities of C_2F_4^+ and C_3F_5^+ , which are the principal electron-impact dissociative ionization products of $c\text{-C}_4\text{F}_8$,¹⁶ represent only a few percent of the total reactive ion composition, suggesting a high degree of dissociation of the parent gas within the discharge.

Figure 4(b) shows the relative ion composition as a function of pressure in pure $c\text{-C}_4\text{F}_8$ discharges. The magnitude of the total ion flux, as well as the fluxes of all significant ionic species except CF_3^+ , decreases from 0.67 to 2.66 Pa (5–20 mTorr). With the exception of CF_3^+ , the relative abundances of the principal ions do not change significantly as a function of pressure in these discharges. The relative increase of the CF_3^+ flux with increasing pressure again suggests a partial contribution to this species from ion-molecule reactions. As with discharges sustained in pure C_2F_6 , substantial fluxes of ions not formed by electron-impact ionization of the parent gas are likewise present in pure $c\text{-C}_4\text{F}_8$ discharges. The combined Si^+/CO^+ flux is consistently the second highest observed.

The energy distributions of three principal ions in pure $c\text{-C}_4\text{F}_8$ discharges at 0.67, 1.33, and 2.66 Pa (5, 10, and 20 mTorr) are shown in the second column of Fig. 3. The average plasma potential, which corresponds to the mean of the IEDs, is slightly higher in pure $c\text{-C}_4\text{F}_8$ discharges than in pure C_2F_6 discharges for similar discharge conditions. At 0.67 Pa (5 mTorr), the IEDs are comparatively broader in $c\text{-C}_4\text{F}_8$ discharges, with an asymmetric saddle structure barely resolved. Both of these characteristics become more pronounced with increasing pressure, mirroring the pressure dependence of the IEDs observed in pure C_2F_6 discharges. The increase in rf sheath modulation as pressure increases can be similarly ascribed to a more confined plasma lowering the ground sheath capacitance. The extent to which the IEDs are broadened is mass dependent, with the lightest ions the most affected by the rf modulation of plasma potential. The broader and more structured IEDs observed in pure $c\text{-C}_4\text{F}_8$ discharges compared to those observed in pure C_2F_6 discharges likely result from higher rates of electron attachment leading to a more confined plasma. Electron attachment to $c\text{-C}_4\text{F}_8$ occurs both at lower energies and with a significantly larger cross section compared to C_2F_6 .¹⁷ In addition, the relative intensities of the low-energy peaks seen in CF_3^+ and CF^+ IEDs are higher in $c\text{-C}_4\text{F}_8$ discharges, indicating increased charge-exchange production of these ions.

C. Ar: C_2F_6 and Ar: $c\text{-C}_4\text{F}_8$ mixtures

The mass analyzed ion flux from discharges containing varying proportions of C_2F_6 and $c\text{-C}_4\text{F}_8$ with Ar is shown in Fig. 5. Although the Ar^+ intensity sharply decreases with the reduction of Ar supplied to the plasma, the relative fluxes of

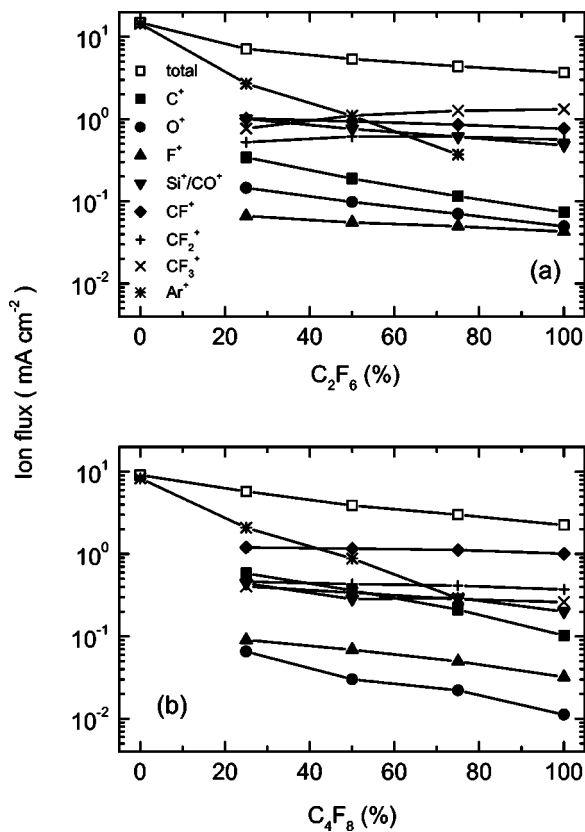


FIG. 5. (a) Mass analyzed ion flux striking the lower electrode of the GEC cell as the (a) C₂F₆ and (b) *c*-C₄F₈ fractions are varied from 0% to 100%. The balance of the feed gas is Ar. Discharge pressure and power are 1.33 Pa (10 mTorr) and 200 W, respectively. The legend applies to both graphs.

all other significant ions in these discharges are largely unaffected by the corresponding increase in the concentration of fluorocarbon gas in the feed mixture. The decrease in the total ion current in both Ar:C₂F₆ and Ar:*c*-C₄F₈ discharges with increasing fluorocarbon concentration is likely due to reduced plasma densities resulting from increasing electron attachment to the fluorocarbon gases and their dissociation products. CF₃⁺ energy distributions measured for these discharge conditions are shown in Fig. 6. As the proportion of either C₂F₆ or *c*-C₄F₈ supplied to the plasma increases, the IEDs widen and begin to exhibit bimodal splitting. Furthermore, in Ar:C₂F₆ discharges, the average plasma potential noticeably increases with the C₂F₆ fraction. It is unclear why a similar increase is not observed in Ar:*c*-C₄F₈ discharges.

The mass analyzed ion flux as a function of pressure for discharges containing equal mixtures of either C₂F₆ or *c*-C₄F₈ with Ar is shown in Fig. 7. For both gas mixtures, the total ion flux decreases with increasing pressure. The reduced ion flux at larger pressures may result from a reduction of electron temperature or increased electron attachment due to increased collisions. Only at the lowest pressure studied is Ar⁺ the dominant ion in 50% Ar:50% C₂F₆ discharges. In 50% Ar:50% *c*-C₄F₈ discharges, CF⁺ rather than Ar⁺ is the dominant ion. Similar to discharges sustained in pure *c*-C₄F₈, C₂F₄⁺ and C₃F₅⁺, the principal products of the dissociative ionization of *c*-C₄F₈ and dissociative charge transfer from

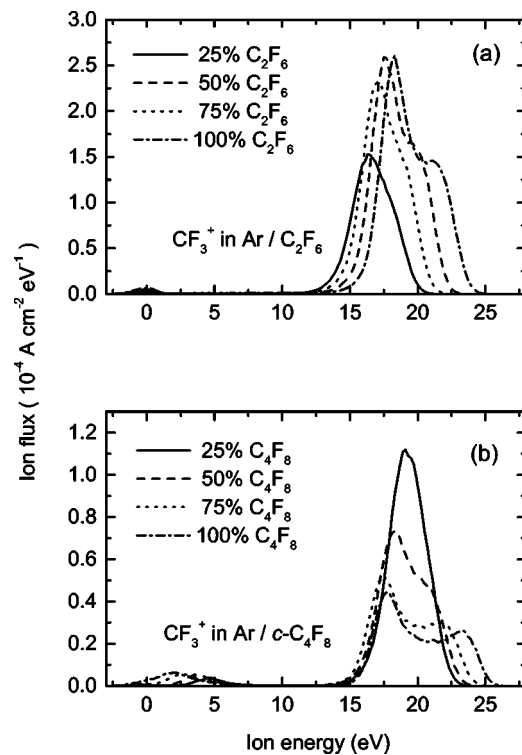


FIG. 6. CF₃⁺ energy distribution as the (a) C₂F₆ and (b) *c*-C₄F₈ fractions are varied from 0% to 100%. The balance of the feed gas is Ar. Discharge pressure and power are 1.33 Pa (10 mTorr) and 200 W, respectively.

Ar⁺ to *c*-C₄F₈,¹⁶ represent only a small fraction of the reactive ion composition in 50% Ar:50% *c*-C₄F₈ discharges.

IV. SUMMARY

Several ionic species with significant intensities were observed in discharges containing C₂F₆ and *c*-C₄F₈. The dominant ion is not always the principal ion resulting from electron-impact ionization of the feed gas, particularly in discharges containing *c*-C₄F₈, suggesting a large degree of dissociation. Ions resulting from erosion of the quartz coupling window and confinement ring constitute significant fractions of the reactive ion composition for these plasmas, under some conditions comprising nearly 40% of the measured ion current. The CF₃⁺ flux rises dramatically as a function of pressure in pure C₂F₆ discharges, contributing to an overall increase in ion current under these circumstances. For all other discharges studied, the CF₃⁺ flux displays a much weaker dependence on discharge pressure, and the total ion flux decreases at elevated pressures as might be expected from a reduction of electron temperature at higher collisional frequencies. Although the Ar⁺ flux displays a dependence on the Ar fraction in the feed gas supply, the relative abundances of the remainder of the reactive ion composition in discharges sustained in mixtures of either C₂F₆ or *c*-C₄F₈ are mostly unaffected by changes in the gas mixture.

Depending on the discharge conditions, the ion energy distributions vary from fairly narrow and single peaked to very broad and bimodally structured, the latter being indicative of parasitic capacitive coupling modulating the ions' en-

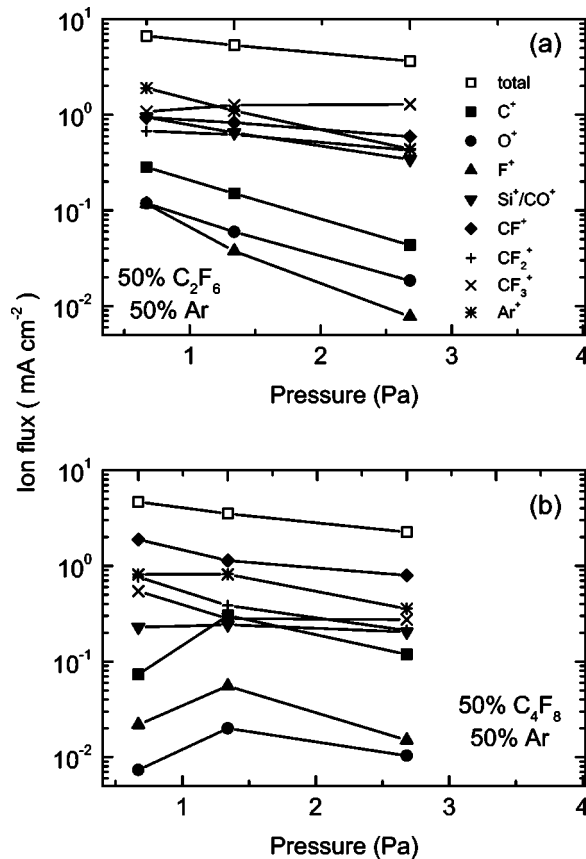


FIG. 7. (a) Mass analyzed ion flux striking the lower electrode of the GEC cell for (a) 50% Ar:50% C_2F_6 and (b) 50% Ar:50% $c-C_4F_8$ discharges as functions of pressure. Discharge power is maintained at 200 W. The legend applies to both graphs.

ergy as they traverse the plasma sheath. The IEDs occurring in pure $c-C_4F_8$ discharges exhibit more pronounced broadening and bimodality than do the corresponding IEDs in pure C_2F_6 discharges for similar discharge conditions. Elevated gas pressures and higher percentages of either C_2F_6 or $c-C_4F_8$ supplied to the discharge were all observed to result in

comparatively broader and more highly bimodal IEDs. The dependence of the IEDs on discharge conditions illustrates the importance of measuring IEDs in determining relative ion flux intensities, since the relative ion flux intensities will depend on the energy of the ions sampled if the IEDs have mass-dependent structure such as those observed in these experiments.

ACKNOWLEDGMENTS

The authors would like to thank Dr. L. G. Christophorou for useful discussions during the preparation of this manuscript. One of the authors (A.N.G.) gratefully acknowledges the support of a National Research Council postdoctoral associateship.

- ¹K. Kurihara and M. Sekino, *Plasma Sources Sci. Technol.* **5**, 121 (1996).
- ²S. Sasaki, Y. Hirose, I. Ishikawa, K. Nagaseki, Y. Saito, and S. Suganomata, *Jpn. J. Appl. Phys., Part 1* **30**, 5296 (1997).
- ³Y. Hirose, I. Ishikawa, S. Sasaki, K. Nagaseki, Y. Saito, and S. Suganomata, *Jpn. J. Appl. Phys., Part 1* **37**, 5730 (1997).
- ⁴R. Jayaraman, R. T. McGrath, and G. A. Hebner, *J. Vac. Sci. Technol. A* **17**, 1545 (1999).
- ⁵X. Li, M. Schaepkens, G. S. Oehrlein, R. E. Ellefson, L. C. Frees, N. Mueller, and N. Korner, *J. Vac. Sci. Technol. A* **17**, 2438 (1999).
- ⁶P. A. Miller, G. A. Hebner, K. E. Greenberg, P. S. Pochan, and B. P. Aragon, *J. Res. Natl. Inst. Stand. Technol.* **100**, 427 (1995).
- ⁷P. J. Hargis *et al.*, *Rev. Sci. Instrum.* **65**, 140 (1994).
- ⁸J. K. Olthoff and K. E. Greenberg, *J. Res. Natl. Inst. Stand. Technol.* **100**, 327 (1995).
- ⁹J. K. Olthoff and Y. Wang, *J. Vac. Sci. Technol. A* **17**, 1552 (1999).
- ¹⁰Y. Wang and J. K. Olthoff, *J. Appl. Phys.* **85**, 6358 (1999).
- ¹¹M. V. S. Rao, R. J. Van Brunt, and J. K. Olthoff, *Phys. Rev. E* **54**, 5491 (1996).
- ¹²C. Q. Jiao, A. Garscadden, and P. D. Haaland, *Chem. Phys. Lett.* **310**, 52 (1999).
- ¹³Y. Wang, M. Misakian, A. N. Goyette, and J. K. Olthoff, *J. Appl. Phys.* (to be published).
- ¹⁴J. Hopwood, *Appl. Phys. Lett.* **62**, 940 (1993).
- ¹⁵J. T. Gudmundsson, *Plasma Sources Sci. Technol.* **8**, 58 (1999).
- ¹⁶C. Q. Jiao, A. Garscadden, and P. D. Haaland, *Chem. Phys. Lett.* **297**, 121 (1998).
- ¹⁷L. G. Christophorou, D. L. McCorkle, and A. A. Christodoulides, in *Electron Attachment Processes*, Vol. 1 of *Electron-Molecule Interactions and Their Applications*, edited by L. G. Christophorou (Academic, Orlando, 1984), Chap. 6, pp. 478–618.